



## Stabilization of a steady state in oscillators coupled by a digital delayed connection

メタデータ	言語: eng 出版者: 公開日: 2020-09-11 キーワード (Ja): キーワード (En): 作成者: Konishi, Keiji, Ba Le, Luan, Hara, Naoyuki メールアドレス: 所属:
URL	<a href="http://hdl.handle.net/10466/00017039">http://hdl.handle.net/10466/00017039</a>

# Stabilization of a steady state in oscillators coupled by a digital delayed connection

Keiji Konishi, Luan Ba Le, and Naoyuki Hara

Department of Electrical and Information Systems, Osaka Prefecture University  
1-1 Gakuen-cho, Naka-ku, Sakai, Osaka 599-8531, Japan

Received: date / Revised version: date

**Abstract.** The present paper deals with stabilization of a steady state in a networked oscillator system that consists of oscillators coupled by a digital delayed connection. This connection is realized by a first-in, first-out queue. The semi-discretization technique allows us to obtain a simple characteristic equation for steady-state stability. This equation can be expressed by real polynomials whose coefficients depend on the network topology. The stability analysis based on the characteristic polynomials reveals that the digital delayed connection better facilitates the stabilization of the steady state compared to the well-known continuous-time delayed connection.

## 1 Introduction

The dynamics of coupled oscillators have been actively investigated in nonlinear science [1–3]. Recently, coupled oscillators have been used for engineering applications such as central pattern generators for robotic-legged locomotion [4], modular robots [5], sensor networks [6], and a car-following model [7]. Diffusive-coupling-induced stabilization of unstable steady states, one of the well-known phenomena in coupled oscillators, has been studied for almost a quarter-century [8,9]. This phenomenon, called amplitude death, has great industrial potential, but never occurs in coupled *identical* oscillators [9,10]. Reddy *et al.* showed that a transmission delay in connections can induce this phenomenon even in coupled identical oscillators [11]. This time-delay-induced death has been widely investigated both experimentally [12–14] and analytically [15,10,16–27]. Furthermore, it was reported that amplitude death can be induced not only by using a simple time-delay connection [11] but also by leveraging various connections such as distributed delay connections [28], dynamic connections [29–31], unsymmetrical time-delay connections [32,33], connections via conjugate variables [34,35], time-varying delay connections [36], two long-delay connections [37], and gradient time-delay connections [38]. These connections represent the *continuous-time* mutual influences of real oscillators for various situations.

In the field of control engineering, a networked control system whose subsystems (i.e., sensors, actuators, and controllers) are communicated through a digital communication network (e.g., Ethernet), as shown in Fig. 1(a), has been extensively investigated. This is because this system has the following advantages: reduced system wiring, ease of system diagnosis and maintenance, and increased system agility [39]. The subsystems communicate with each

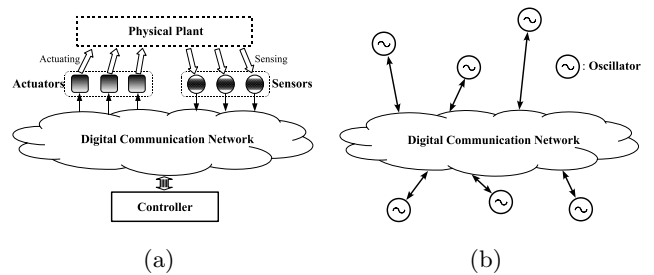


**Fig. 1.** Conceptual diagrams of networked systems: (a) networked control system; (b) networked oscillator system.

other on the network by digital signals that are converted from continuous-time input–output signals of subsystems. Note that a communication delay, which may degrade the system performance, is inevitably caused by the signal transmission on the network. From the viewpoint of the engineering applications of coupled oscillators, it is important to investigate the dynamics of oscillators that are coupled through the digital communication network. We call such configuration a networked oscillator system, as illustrated in Fig. 1(b). To the best of our knowledge, few studies have been so far conducted on networked oscillator systems in the field of nonlinear dynamics.

The present paper proposes a prototype model of a networked oscillator system that consists of oscillators coupled by a digital delayed connection. Figure 2 sketches the prototype model with two oscillators, where the digital delayed connection is implemented by the first-in, first-out (FIFO) queues. The main purpose of this study is to investigate amplitude death induced by the digital de-

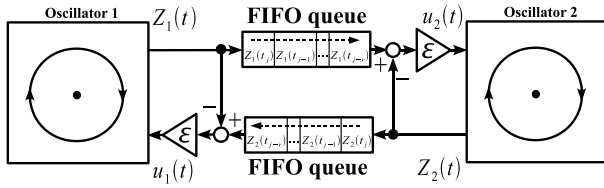


**Fig. 2.** Block diagram of two oscillators coupled by a digital delayed connection (i.e., FIFO queues).

laid connection. The semi-discretization technique [40–43] allows us to derive a simple characteristic equation for steady-state stability. This equation can be expressed by real polynomials whose coefficients depend on the network topology. The stability analysis reveals that the digital delayed connection better facilitates the stabilization of the steady state compared to the continuous-time delayed connection.

## 2 Coupled oscillators

A network consisting of two-dimensional oscillators,

$$\dot{Z}_n(t) = \{\mu + i\omega - |Z_n(t)|^2\} Z_n(t) + \varepsilon u_n(t) \quad (n = 1, 2, \dots, N), \quad (1)$$

is considered, where the complex number  $Z_n(t) \in \mathbf{C}$  is the state variable of oscillator  $n$ .  $N \geq 2$  denotes the total number of oscillators. The parameters  $\mu > 0$  and  $\omega > 0$  represent the degree of instability of the fixed point and the oscillator frequency, respectively.  $\varepsilon \in \mathbf{R}$  is the coupling strength and  $i$  is denoted as  $i = \sqrt{-1}$ . For a normal delayed connection, the coupling signal  $u_n(t) \in \mathbf{C}$  is given by

$$u_n(t) = \frac{1}{d_n} \left[ \sum_{k=1}^N c_{nk} Z_k(t - \tau) \right] - Z_n(t), \quad (2)$$

where  $\tau \geq 0$  is the delay time of the coupling signals. The network topology is governed by  $c_{nk}$  as follows: if oscillator  $n$  is connected to oscillator  $k$ , then  $c_{nk} = c_{kn} = 1$ , otherwise  $c_{nk} = c_{kn} = 0$ . The self-delayed signal  $Z_n(t - \tau)$  is not allowed to be injected, that is,  $c_{nn} = 0$ . The number of oscillators that are connected to oscillator  $n$ , denoted as the degree of oscillator  $n$ , is written as  $d_n := \sum_{k=1}^N c_{nk}$ . Suppose that there is no isolated oscillator, that is,  $d_n > 0, \forall n \in \{1, \dots, N\}$ .

Instead of normal delayed connection (2), the present study employs the digital delayed connection

$$u_n(t) = \frac{1}{d_n} \left[ \sum_{k=1}^N c_{nk} Z_k(t_{j-r}) \right] - Z_n(t) \quad (3)$$

for  $t \in [t_j, t_{j+1})$  ( $j = 0, 1, \dots$ ). Figure 2 illustrates the two oscillators coupled by digital delayed connection (3). As shown in Figs. 2 and 3,  $Z_k(t)$  is periodically stored with sampling period  $h := t_{j+1} - t_j$  into the buffers on the

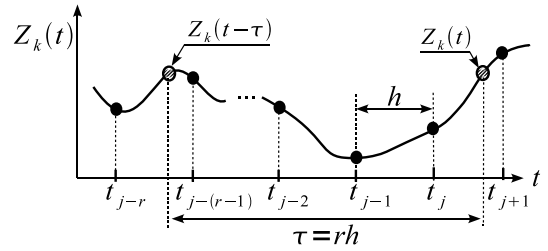


**Fig. 3.** Sketch of state variable  $Z_k(t)$  for oscillator  $k$ .

FIFO queue, where  $j$  represents the sampling number.  $t_j$  denotes the time at  $j$ -th sampling.  $Z_k(t_{j-r}) := Z_k(t_j - rh)$  is the past state variable, which is maintained at a constant value during  $t \in [t_j, t_{j+1})$ . The integer  $(r + 1)$  is the number of buffers; thus, the time delay is given by  $\tau = rh$ .

It may be worth pointing out the following remarks on these connections. In the case of a single oscillator (i.e.,  $N = 1, c_{11} = 1$ , and  $d_1 = 1$ ), oscillator (1) with normal delayed feedback (2) and that with digital delayed feedback (3) are identical to the original delayed feedback control system [44] and the queue-based delayed feedback control system [45], respectively. Connection (3), with both a large number of buffers and a short sampling period (i.e.,  $1 \ll r$  and  $h \ll 1$ ), is approximately identical to normal delayed connection (2). In the field of nonlinear science, a delayed signal is often realized by a bucket brigade delay (BBD) line device in experimental situations [46–48, 12, 49, 14]. Such a device comprises a series of sample-and-hold circuits. The BBD line device is also described by the FIFO queue; thus, the coupled oscillators in Fig. 2 are identical to the oscillators coupled by the BBD line [12].

## 3 Stability analysis

Oscillators (1) with connection (3) have the homogeneous steady state  $\mathbf{Z}^* := [0 \ 0 \ \dots \ 0]^T \in \mathbf{C}^N$ . The coupled oscillators are linearized around  $\mathbf{Z}^*$ :

$$\dot{z}_n(t) = (\mu + i\omega) z_n(t) + \varepsilon \left[ \left\{ \frac{1}{d_n} \sum_{k=1}^N c_{nk} z_k(t_{j-r}) \right\} - z_n(t) \right] \quad (4)$$

for  $t \in [t_j, t_{j+1})$  ( $j = 0, 1, \dots$ ), where  $z_n(t) \in \mathbf{C}$  is the variation in oscillator  $n$  around the fixed point  $Z_n^* = 0$ . System (4) can be written by

$$\dot{\mathbf{x}}(t) = \mathbf{A}\mathbf{x}(t) + \mathbf{B}\mathbf{x}(t_{j-r}), \quad t \in [t_j, t_{j+1}) \quad (j = 0, 1, \dots), \quad (5)$$

where

$$\mathbf{x}(t) := [\text{Re}\{z_1(t)\} \ \text{Im}\{z_1(t)\} \ \dots \ \text{Re}\{z_N(t)\} \ \text{Im}\{z_N(t)\}]^T, \quad (6)$$

$$\mathbf{A} := \mathbf{I}_N \otimes \begin{bmatrix} \mu - \varepsilon & -\omega \\ \omega & \mu - \varepsilon \end{bmatrix}, \quad \mathbf{B} := \varepsilon \mathbf{D} \otimes \mathbf{I}_2. \quad (7)$$

The elements of matrix  $\mathbf{D} \in \mathbf{R}^{N \times N}$  are  $\{\mathbf{D}\}_{nk} := c_{nk}/d_n$  for  $n \neq k$  and  $\{\mathbf{D}\}_{nn} := 0$ . Here an  $N$ -dimensional identity matrix is represented by  $\mathbf{I}_N$ .

The semi-discretization technique [40–43] allows us to derive the mapping from the past state  $\mathbf{x}(t_{j-r})$  and the current state  $\mathbf{x}(t_j)$  to the future state  $\mathbf{x}(t_{j+1})$ ,

$$\mathbf{x}(t_{j+1}) = \mathbf{L}_a \mathbf{x}(t_j) + \mathbf{L}_b \mathbf{x}(t_{j-r}),$$

where

$$\mathbf{L}_a := \exp\{\mathbf{A}h\}, \quad \mathbf{L}_b := \exp\{\mathbf{A}h\} \int_0^h \exp\{-\mathbf{A}s\} ds \mathbf{B}. \quad (8)$$

This mapping implies that the dynamics of linear system (5) can be reduced to that of a  $2(r+1)N$ -dimensional discrete-time system,

$$\mathbf{X}_{j+1} = \Phi \mathbf{X}_j, \quad (9)$$

where

$$\mathbf{X}_j := \begin{bmatrix} \mathbf{x}(t_j) \\ \mathbf{x}(t_{j-1}) \\ \mathbf{x}(t_{j-2}) \\ \vdots \\ \mathbf{x}(t_{j-r}) \end{bmatrix}, \quad \Phi := \begin{bmatrix} \mathbf{L}_a & \mathbf{0} & \cdots & \mathbf{0} & \mathbf{L}_b \\ \mathbf{I}_{2N} & \mathbf{0} & \cdots & \mathbf{0} & \mathbf{0} \\ \mathbf{0} & \mathbf{I}_{2N} & \cdots & \mathbf{0} & \mathbf{0} \\ \vdots & & \ddots & & \vdots \\ \mathbf{0} & \mathbf{0} & \cdots & \mathbf{I}_{2N} & \mathbf{0} \end{bmatrix}.$$

Note that  $\mathbf{Z}^*$  is stable if and only if the transition matrix  $\Phi$  is a stable matrix (i.e., Schur matrix).

The characteristic polynomial of linear system (9) is described by

$$\begin{aligned} g(\lambda) &= \det(\lambda \mathbf{I}_{2(r+1)N} - \Phi) \\ &= \det(\mathbf{H}) \\ &= \det \left\{ \lambda \mathbf{I}_{2N} - \mathbf{L}_a - [\mathbf{0} \ \mathbf{0} \ \cdots \ -\mathbf{L}_b] \mathbf{H}^{-1} \begin{bmatrix} -\mathbf{I}_{2N} \\ \mathbf{0} \\ \vdots \\ \mathbf{0} \end{bmatrix} \right\}, \end{aligned}$$

where  $\mathbf{H} \in \mathbf{R}^{2rN \times 2rN}$  is given by

$$\mathbf{H} := \begin{bmatrix} \lambda \mathbf{I}_{2N} & \mathbf{0} & \cdots & \mathbf{0} & \mathbf{0} \\ -\mathbf{I}_{2N} & \lambda \mathbf{I}_{2N} & & \mathbf{0} & \mathbf{0} \\ \mathbf{0} & -\mathbf{I}_{2N} & & \mathbf{0} & \mathbf{0} \\ \vdots & & \ddots & \ddots & \vdots \\ \mathbf{0} & \mathbf{0} & \cdots & -\mathbf{I}_{2N} & \lambda \mathbf{I}_{2N} \end{bmatrix}.$$

Now  $\mathbf{P} \in \mathbf{R}^{2N \times 2N}$  is denoted by

$$\mathbf{H}^{-1} = \begin{bmatrix} * & * \\ \mathbf{P} & * \end{bmatrix}. \quad (10)$$

As  $\det(\mathbf{H}) = \lambda^{2rN}$  and  $\mathbf{P} = \lambda^{-r} \mathbf{I}_{2N}$ , polynomial  $g(\lambda)$  can be further simplified to

$$g(\lambda) = \det\{\lambda^{r+1} \mathbf{I}_{2N} - \lambda^r \mathbf{L}_a - \mathbf{L}_b\}. \quad (11)$$

Let us calculate Eq. (11) below. Substituting  $\mathbf{A}$  and  $\mathbf{B}$  in Eq. (7) into  $\mathbf{L}_a$  and  $\mathbf{L}_b$  denoted in Eq. (8), we obtain

$$\mathbf{L}_a = \gamma \mathbf{I}_N \otimes \Theta(h), \quad \mathbf{L}_b = \eta (\mathbf{I}_N - \mathbf{M}) \otimes \mathbf{Q} (\gamma \Theta(h) - \mathbf{I}_2),$$

where

$$\gamma := e^{(\mu-\varepsilon)h}, \quad \eta := \frac{\varepsilon}{\omega^2 + (\mu-\varepsilon)^2}, \quad \mathbf{M} := \mathbf{I}_N - \mathbf{D}, \quad (12)$$

$$\Theta(h) := \begin{bmatrix} \cos \omega h & -\sin \omega h \\ \sin \omega h & \cos \omega h \end{bmatrix}, \quad \mathbf{Q} := \begin{bmatrix} \mu - \varepsilon & \omega \\ -\omega & \mu - \varepsilon \end{bmatrix}. \quad (13)$$

Since  $\mathbf{M}$  is self-adjoint and positive semidefinite [18,19], it can be diagonalized as  $\mathbf{T}^{-1} \mathbf{M} \mathbf{T} = \text{diag}(\rho_1, \rho_2, \dots, \rho_N)$ , where  $\mathbf{T}$  is a diagonal transformation matrix and  $\rho_q$  ( $q = 1, 2, \dots, N$ ) are the eigenvalues of  $\mathbf{M}$ . Therefore, we obtain

$$\begin{aligned} g(\lambda) &= \det\{(\mathbf{T}^{-1} \otimes \mathbf{I}_2) (\lambda^{r+1} \mathbf{I}_{2N} - \lambda^r \mathbf{L}_a - \mathbf{L}_b) (\mathbf{T} \otimes \mathbf{I}_2)\} \\ &= \det\{(\lambda^{r+1} \mathbf{I}_{2N} - \lambda^r \gamma \mathbf{I}_N \otimes \Theta(h) - \eta (\mathbf{T}^{-1} \otimes \mathbf{I}_2) (\mathbf{I}_N - \mathbf{M}) \otimes \mathbf{Q} (\gamma \Theta(h) - \mathbf{I}_2) (\mathbf{T} \otimes \mathbf{I}_2))\} \\ &= \det\{(\lambda^{r+1} \mathbf{I}_{2N} - \lambda^r \gamma \mathbf{I}_N \otimes \Theta(h) - \eta (\mathbf{I}_N - \mathbf{T}^{-1} \mathbf{M} \mathbf{T}) \otimes \mathbf{Q} (\gamma \Theta(h) - \mathbf{I}_2))\} \\ &= \det\{(\lambda^{r+1} \mathbf{I}_{2N} - \lambda^r \gamma \mathbf{I}_N \otimes \Theta(h) - \eta (\mathbf{I}_N - \text{diag}(\rho_1, \rho_2, \dots, \rho_N)) \otimes \mathbf{Q} (\gamma \Theta(h) - \mathbf{I}_2))\}. \end{aligned} \quad (14)$$

As a result,  $g(\lambda) = 0$  can be expressed as

$$g(\lambda) = \prod_{q=1}^N \bar{g}(\lambda, \rho_q) = 0, \quad (15)$$

$$\bar{g}(\lambda, \rho_q) = \det\{\lambda^{r+1} \mathbf{I}_2 - \lambda^r \gamma \Theta(h) - \eta (1 - \rho_q) \mathbf{Q} (\gamma \Theta(h) - \mathbf{I}_2)\}. \quad (16)$$

The function  $\bar{g}(\lambda, \rho_q)$  can be described by the following  $2(r+1)$ -degree polynomial:

$$\begin{aligned} \bar{g}(\lambda, \rho_q) &= \lambda^{2(r+1)} + \alpha_4 \lambda^{2r+1} + \alpha_3 \lambda^{2r} \\ &\quad + \alpha_2(\rho_q) \lambda^{r+1} + \alpha_1(\rho_q) \lambda^r + \alpha_0(\rho_q), \end{aligned} \quad (17)$$

where

$$\begin{aligned} \alpha_0(\rho_q) &:= (1 - \rho_q)^2 \varphi_0, \quad \alpha_1(\rho_q) := (1 - \rho_q) \varphi_1, \\ \alpha_2(\rho_q) &:= (1 - \rho_q) \varphi_2, \quad \alpha_3 := \gamma^2, \quad \alpha_4 := -2\gamma \cos \omega h. \end{aligned}$$

The parameters  $\varphi_0$ ,  $\varphi_1$ , and  $\varphi_2$  are defined by

$$\begin{aligned} \varphi_0 &:= \eta^2 (\gamma^2 - 2\gamma \cos \omega h + 1) \{\omega^2 + (\mu - \varepsilon)^2\}, \\ \varphi_1 &:= 2\eta \gamma \{(\mu - \varepsilon)(\gamma - \cos \omega h) + \omega \sin \omega h\}, \\ \varphi_2 &:= -2\eta \{(\mu - \varepsilon)(\gamma \cos \omega h - 1) + \omega \gamma \sin \omega h\}, \end{aligned}$$

respectively. The homogeneous steady state  $\mathbf{Z}^*$  of the coupled oscillators on network topology  $\mathbf{D}$  is stable if and only if all the roots  $\lambda$  of  $\bar{g}(\lambda, \rho_q) = 0$  ( $q = 1, 2, \dots, N$ ) lie within the unit circle on the complex plane.

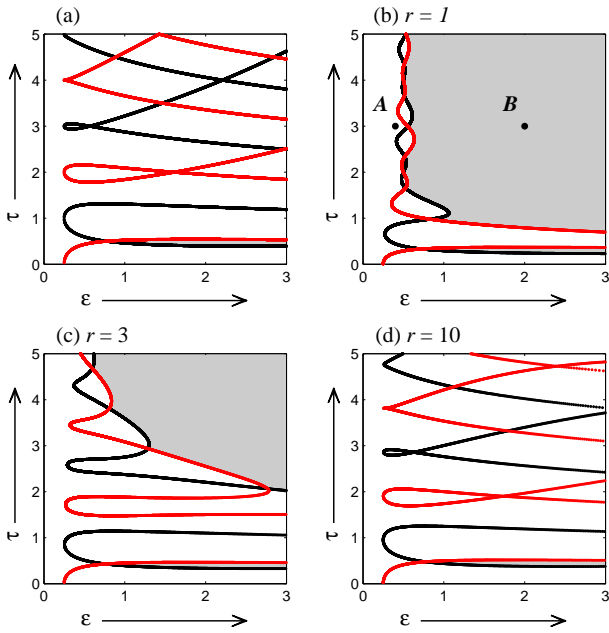


**Fig. 4.** Marginal stability curves for a pair of oscillators ( $N = 2, \mu = 0.5, \omega = \pi$ ): (a) normal delayed connection (2), (b) – (d) digital delayed connection (3) ( $r = 1, 3, 10$ ). Black and red curves correspond to  $\rho_1 = 0$  and  $\rho_2 = 2$ , respectively. The stability regions are represented by shaded areas.

## 4 Numerical examples

This section investigates the stability regions in the connection parameter space  $\varepsilon - \tau$  for the networked oscillator system on some typical network topologies. The marginal stability curves are estimated to obtain these regions. The following steps are used for the estimation: (i) number of oscillators,  $N$ , and network topology  $c_{nk}$  are given; (ii) eigenvalues  $\rho_q$  of matrix  $\mathbf{M}$ , as denoted in Eq. (12), are calculated; (iii)  $\bar{g}(e^{i\theta}, \rho_q) = g_R(\theta, \rho_q) + ig_I(\theta, \rho_q)$  is derived; (iv) marginal stability curves are estimated by solving  $g_R(\theta, \rho_q) = 0$  and  $g_I(\theta, \rho_q) = 0$  for  $\theta \in [0, \pi]$ .

### 4.1 A pair of oscillators ( $N = 2$ )

Let us now focus on the simplest case, a pair of oscillators (i.e.,  $N = 2$ ) illustrated in Fig. 2. The eigenvalues of  $\mathbf{M}$  are  $\rho_1 = 0$  and  $\rho_2 = 2$ . The marginal stability curves are shown in Figs. 4 (a) – (d). Figure 4 (a) presents the curves with normal delayed connection (2), which are estimated by solving

$$\bar{g}(i\lambda_I, \rho_q) := i\lambda_I - \mu + \varepsilon - i\omega - \varepsilon e^{-i\lambda_I \tau} (1 - \rho_q) = 0, \quad \lambda_I \in \mathbf{R}, \quad (18)$$

with  $\rho_1 = 0$  and  $\rho_2 = 2$  (for more details, see our previous paper [37]). There exists a thin stability region at around  $\tau \approx 0.5$ . The curves with digital delayed connection (3) for  $r = 1, 3, 10$  are shown in Figs. 4 (b) – (d), respectively. For small numbers of buffers,  $r = 1$  and 3, the stability regions become much larger compared with

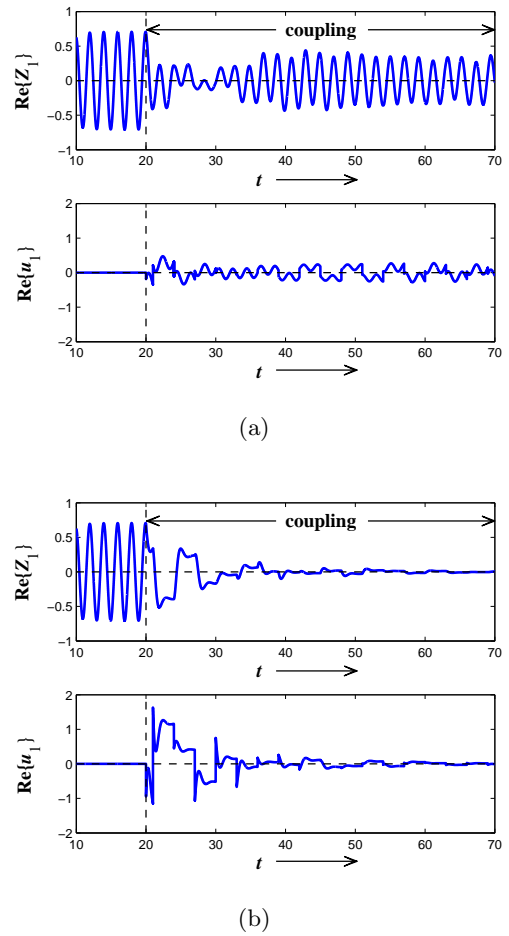


**Fig. 5.** Time-series data,  $\text{Re}\{Z_1\}$  and  $\text{Re}\{u_1\}$ , for a pair of oscillators coupled by digital delayed connection (3) ( $N = 2, \mu = 0.5, \omega = \pi, r = 1$ ): (a)  $\varepsilon = 0.3$  and  $\tau = 3$  (i.e., A in Fig. 4 (b)), (b)  $\varepsilon = 2.0$  and  $\tau = 3$  (i.e., B in Fig. 4 (b)).

those of the normal connection. On the other hand, for a large number  $r = 10$ , the curves closely resemble those of the normal connection. This result is exemplified by the fact that digital connection (3) with  $1 \ll r$  and  $h \ll 1$  is approximately identical to normal connection (2).

Time-series data of real parts of  $Z_1$  and  $u_1$ , i.e.,  $\text{Re}\{Z_1\}$  and  $\text{Re}\{u_1\}$ , with  $r = 1$  at the parameter sets A and B in Fig. 4 (b) are plotted in Figs. 5(a) and 5(b), respectively. A pair of oscillators behave independently and are then coupled by the digital connection at  $t = 20$ . For the parameter set A,  $\text{Re}\{Z_1\}$  and  $\text{Re}\{u_1\}$  continue to oscillate even after coupling; that is, the connection fails to stabilize the steady state. In contrast, for the parameter set B, the connection succeeds in stabilizing it:  $\text{Re}\{Z_1\}$  and  $\text{Re}\{u_1\}$  converge to zero after coupling. These numerical results agree with our analytical results depicted in Fig. 4.

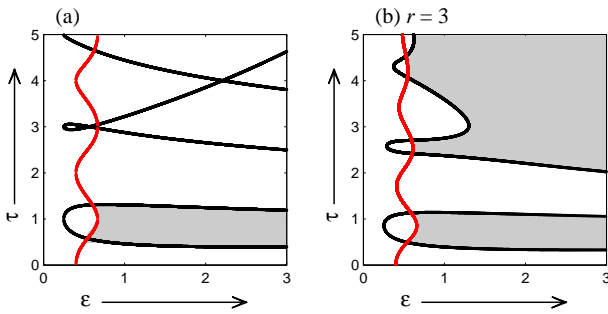


**Fig. 6.** Marginal stability curves for a complete network ( $N = 5, \mu = 0.5, \omega = \pi$ ): (a) normal delayed connection (2), (b) digital delayed connection (3) with  $r = 3$ . Black and red curves correspond to  $\rho_1 = 0$  and  $\rho_{2,3,4,5} = 5/4$ , respectively. The stability regions are represented by shaded areas.

## 4.2 Networked oscillators ( $N = 5$ )

Here we consider five oscillators on two typical network topologies, the complete network (i.e., all-to-all connections) and the ring network (i.e., chain connection with periodic boundary). The eigenvalues of  $\mathbf{M}$  for the complete network are  $\rho_1 = 0$  and  $\rho_{2,3,4,5} = 5/4$ . The marginal stability curves for normal connection (2), which are estimated by solving Eq. (18) with  $\rho_{1\sim 5}$ , are shown in Fig. 6 (a). The stability region exists at around  $\tau \approx 1.0$ . Figure 6 (b) illustrates the curves for digital connection (3) with  $r = 3$ . It can be seen that there exists a large stability region with  $\tau \gtrsim 2.0$ : the stability regions become much larger compared with that of the normal connection.

For the ring network, the eigenvalues of  $\mathbf{M}$  are  $\rho_1 = 0$ ,  $\rho_{2,3} = 0.691$ , and  $\rho_{4,5} = 1.809$ . Figure 7 (a) shows the marginal stability curves for normal connection (2) on the ring network. We see the stability region with  $0.5 \lesssim \tau \lesssim 1.3$ . The curves for digital connection (3) with  $r = 3$  are shown in Fig. 7 (b). There exists a large stability region with  $\tau \gtrsim 2.0$ : the stability regions become much larger compared with that of the normal connection, as is the case in the complete network.

From these numerical results shown in Figs. 4, 6, and 7, it may be concluded that the digital delayed connection better facilitates stabilization compared to the continuous-time delayed connection. Remark that this conclusion is consistent with paper [43] showing that digital delayed feedback signals facilitate stabilization compared to the continuous-time delayed feedback.

## 5 Discussions and Conclusion

Let us discuss the influence of network topology and number of buffers on stability. According to characteristic equation (15), the stability of steady state  $\mathbf{Z}^*$  depends on the eigenvalues  $\rho_q$  ( $q = 1, \dots, N$ ) of  $\mathbf{M}$ . This fact leads to a conclusion that the network topology does not have direct influence on stability; for example, two different networks which have the same  $\rho_q$  have the same stability region. Although this is valid only for the local stability, we think

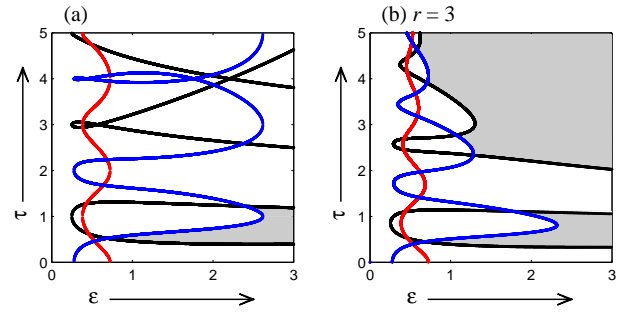


**Fig. 7.** Marginal stability curves for a ring network ( $N = 5, \mu = 0.5, \omega = \pi$ ): (a) normal delayed connection (2), (b) digital delayed connection (3) with  $r = 3$ . Black, red, and blue curves correspond to  $\rho_1 = 0$ ,  $\rho_{2,3} = 0.691$ , and  $\rho_{4,5} = 1.809$ , respectively. The stability regions are represented by shaded areas.

that the transient behavior far from the steady state might be influenced by not only  $\rho_q$  but also the network topology. The transient behavior needs further consideration.

From our numerical results shown in Fig. 4, it can be seen that the number of buffers,  $r$ , has a strong influence on the stability. We numerically observed that the stability region tends to be large for a small number of buffers. However, the theoretical relation between the number and the stability region cannot be obtained. There is room for argument on this point.

The present paper has investigated the stability of the steady state in oscillators coupled by the digital delayed connection. Such a connection is described by a FIFO queue. A simple characteristic equation for steady-state stability, with real polynomials whose coefficients depend on the network topology, is derived by the semi-discretization technique. Some numerical results have proved that the digital delayed connection better facilitates stabilization compared to the well-known continuous-time delayed connection.

## Acknowledgments

This study was partially supported by JSPS KAKENHI (23560538) and the Research Foundation for the Electrotechnology of Chubu.

## References

1. T. Endo, S. Mori, IEEE T. Circuits Syst. **23**, 100 (1976)
2. Y. Nishio, A. Ushida, IEEE T. Circuits Syst. I **42**, 678 (1995)
3. A. Pikovsky, M. Rosenblum, J. Kurths, *Synchronization* (Cambridge University Press, 2001)
4. P. Holmes, R. Full, D. Koditschek, J. Guckenheimer, SIAM Rev. **48**, 207 (2006)
5. A. Ishiguro, M. Shimizua, T. Kawakatsu, Robot. Auton. Syst. **54**, 641 (2006)
6. Y. Hong, A. Scaglione, IEEE J. Sel. Area. in Comm. **23**, 1085 (2005)

7. G. Orosz, G. Stepan, Proc. R. Soc. A. **462**, 2643 (2006)
8. Y. Yamaguchi, H. Shimizu, Physica D **11**, 212 (1984)
9. D. Aronson, G. Ermentout, N. Kopell, Physica D **41**, 403 (1990)
10. K. Konishi, Phys. Lett. A **341**, 401 (2005)
11. D. Reddy, A. Sen, G. Johnston, Phys. Rev. Lett. **80**, 5109 (1998)
12. D. Reddy, A. Sen, G. Johnston, Phys. Rev. Lett. **85**, 3381 (2000)
13. R. Herrero, M. Figueras, J. Rius, F. Pi, G. Orriols, Phys. Rev. Lett. **84**, 5312 (2000)
14. K. Konishi, K. Senda, H. Kokame, Phys. Rev. E **78**, 056216 (2008)
15. D. Reddy, A. Sen, G. Johnston, Physica D **129**, 15 (1999)
16. K. Konishi, Phys. Rev. E **67**, 017201 (2003)
17. F.M. Atay, Physica D **183**, 1 (2003)
18. F.M. Atay, J. Differ. Equations **221**, 190 (2006)
19. F.M. Atay, O. Karabacak, SIAM J. Appl. Dyn. Syst. **5**, 508 (2006)
20. C.-Y. Cheng, Phys. Lett. A **374**, 178 (2009)
21. K. Konishi, Phys. Rev. E **70**, 066201 (2004)
22. R. Dodla, A. Sen, G. Johnston, Phys. Rev. E **69**, 056217 (2004)
23. M. Mehta, A. Sen, Phys. Lett. A **355**, 202 (2006)
24. J. Yang, Phys. Rev. E **76**, 016204 (2007)
25. W. Michiels, H. Nijmeijer, Chaos **19**, 033110 (2009)
26. R. Karnatak, N. Punetha, A. Prasad, R. Ramaswamy, Phys. Rev. E **82**, 046219 (2010)
27. J.M. Höfener, G. C. Sethia, T. Gross, Europhys. Lett. **95**, 40002 (2011)
28. F.M. Atay, Phys. Rev. Lett. **91**, 094101 (2003)
29. K. Konishi, Phys. Rev. E **68**, 067202 (2003)
30. K. Konishi, Int. J. Bifurcations Chaos **17**, 2781 (2007)
31. K. Konishi, N. Hara, Phys. Rev. E **83**, 036204 (2011)
32. Y. Song, J. Wei, Y. Yuan, J. Nonlinear Sci. **17**, 145 (2007)
33. W. Zou, M. Zhan, Phys. Rev. E **80**, 065204 (2009)
34. R. Karnatak, R. Ramaswamy, A. Prasad, Phys. Rev. E **76**, 035201 (2007)
35. T. Singla, N. Pawar, P. Parmananda, Phys. Rev. E **83**, 026210 (2011)
36. K. Konishi, H. Kokame, N. Hara, Phys. Lett. A **374**, 733 (2010)
37. K. Konishi, H. Kokame, N. Hara, Phys. Rev. E **81**, 016201 (2010)
38. W. Zou, C. Yao, M. Zhan, Phys. Rev. E **82**, 056203 (2010)
39. W. Zhang, M.S. Branicky, S.M. Phillips, IEEE Contr. Syst. Mag. **21**, 84 (2001)
40. T. Insperger, G. Stepan, Int. J. Numer. Meth. Eng. **55**, 503 (2002)
41. F. Hartung, T. Insperger, G. Stepan, J. Turi, Appl. Math. Comput. **174**, 51 (2006)
42. T. Insperger, G. Stepan, J. Turi, J. Sound Vib. **313**, 334 (2008)
43. T. Insperger, G. Stepan, J. Turi, Phil. Trans. R Soc. A **368**, 469 (2010)
44. P. Hövel, E. Schöll, Phys. Rev. E **72**, 046203 (2005)
45. K. Konishi, N. Hara, Dyn. Con. Discr. Impul. Sys. B **18**, 679 (2011)
46. P. Celka, Int. J. Bifurcations Chaos **4**, 1703 (1994)
47. T. Imai, K. Konishi, H. Kokame, K. Hirata, Int. J. Bifurcations Chaos **12**, 2897 (2002)
48. A. Kittel, et al., Z. Naturforsch **49a**, 843 (1994)
49. H. Voss, Int. J. Bifurcations Chaos **12**, 1619 (2002)